Carbohydrate Polymers 320 (2023) 121203

Contents lists available at ScienceDirect

Carbohydrate Polymers

journal homepage: www.elsevier.com/locate/carbpol

First transcriptomic insight into the reprogramming of human macrophages by levan-type fructans

Ella Peled [a], Selay Tornaci [b], Ivan Zlotver [a], Arita Dubnika [c,d], Ebru Toksoy Öner [b], Alejandro Sosnik [a,*]

[a] Laboratory of Pharmaceutical Nanomaterials Science, Department of Materials Science and Engineering, Technion – Israel Institute of Technology, Haifa, Israel
[b] IBSB, Department of Bioengineering, Marmara University, Istanbul, Turkey
[c] Faculty of Materials Science and Applied Chemistry, Riga Technical University, Riga, Latvia
[d] Baltic Biomaterials Centre of Excellence, Headquarters at Riga Technical University, Riga, Latvia

ARTICLE INFO

Keywords:
Immunotherapy
Macrophage polarization
Classical (M1) and alternative (M2) macrophage activation
Halomonas levan
Fructan
RNA-seq

ABSTRACT

Based on stimuli in the biological milieu, macrophages can undergo classical activation into the M1 pro-inflammatory (anti-cancer) phenotype or to the alternatively activated M2 anti-inflammatory one. Drug-free biomaterials have emerged as a new therapeutic strategy to modulate macrophage phenotype. Among them, polysaccharides polarize macrophages to M1 or M2 phenotypes based on the surface receptors they bind. Levan, a fructan, has been proposed as a novel biomaterial though its interaction with macrophages has been scarcely explored. In this study, we investigate the interaction of non-hydrolyzed and hydrolyzed *Halomonas* levan and its sulfated derivative with human macrophages in vitro. Viability studies show that these levans are cell compatible. In addition, RNA-sequencing analysis reveals the upregulation of pro-inflammatory pathways. These results are in good agreement with real time-quantitative polymerase chain reaction that indicates higher expression levels of C-X-C Motif Chemokine Ligand 8 and interleukin-6 genes and the M2-to-M1 reprogramming of these cells upon levan treatment. Finally, cytokine release studies confirm that hydrolyzed levans increase the secretion of pro-inflammatory cytokines and reprogram IL-4-polarized macrophages to the M1 state. Overall findings indicate that *Halomonas* levans trigger a classical macrophage activation and pave the way for their application in therapeutic interventions requiring a pro-inflammatory phenotype.

1. Introduction

Macrophages are a critical component of the immune system and are ubiquitously distributed throughout the body, playing a crucial role in homeostasis. Their high plasticity enables them to regulate innate and adaptive immune responses by recruiting other cells, including fibroblasts and lymphocytes. Macrophages demonstrate a spectrum of phenotypes, and their physiological function is dynamically modulated in response to various stimuli present in their microenvironment (Correa-Gallegos et al., 2021; Locati et al., 2020; Yunna et al., 2020). Pro-inflammatory signals such as interferon-γ (IFN-γ) and microbial lipopolysaccharides (LPS) trigger the 'classical' activation into the pro-inflammatory M1 phenotype (Wang, Smith, et al., 2019) and the release of pro-inflammatory (and anti-cancer) cytokines. Conversely, other signals such as interleukin-4 (IL-4) induce 'alternative' macrophage into the anti-inflammatory M2 phenotype that leads to the release of anti-inflammatory cytokines (He et al., 2021; Yunna et al., 2020) and it is involved in tissue repair and regeneration. Depending on microenvironmental stimuli, macrophages can switch between states, a phenomenon known as macrophage reprogramming (Liu et al., 2021; Murray, 2017; Murray et al., 2014; Sica & Mantovani, 2012; Tardito et al., 2019).

Drugs have been investigated to modulate the macrophage phenotype and interfere with different pathophysiological conditions such as cancer, and inflammatory and infectious diseases, though they are often associated with off-target toxicity. Thus, the effect of drug-free biomaterials on macrophage activation has been increasingly investigated. Polysaccharides are among the most biologically active polymers, and they have been shown to differentially modulate macrophage phenotype and reprogramming based on their physicochemical, structural, and

* Corresponding author at: Department of Materials Science and Engineering, Technion – Israel Institute of Technology, De-Jur Building, Office 607, Technion City, 3200003 Haifa, Israel.
E-mail address: sosnik@technion.ac.il (A. Sosnik).

https://doi.org/10.1016/j.carbpol.2023.121203
Received 24 March 2023; Received in revised form 10 July 2023; Accepted 11 July 2023
Available online 13 July 2023

mechanical features (Andrade et al., 2021; Li et al., 2022; Miao et al., 2017; Sridharan et al., 2015; Wang et al., 2022; Wei et al., 2019). This ability stems from their binding to a plethora of surface receptors (Li & Bratlie, 2021). Among them, sulfated glycosaminoglycans such as chondroitin sulfate, dermatan sulfate, heparan sulfate and heparin trigger an M1 polarization through Toll-like receptor 4 (TLR4). Conversely, hyaluronic acid could promote M1 or M2 phenotypes (Li & Bratlie, 2021). Recently, we showed that hydrolyzed galactomannan-based nanoparticles trigger the M2-polarization and the M1-to-M2 reprogramming of murine macrophages in vitro (Peled & Sosnik, 2021).

Levan is a fructose homopolysaccharide (fructan) displaying an uncommon structure consisting of almost only fructosyl residues linked via the β-(2,6) bonds (Scheme 1A) (Toksoy Öner et al., 2016).

The functional properties of levan, including its ability to form spherical self-assembled nanostructures and gels, make it an attractive biomaterial for applications such as drug delivery, cell culture and tissue engineering (Combie & Toksoy Öner, 2018; Kirtel & Öner, 2021). Over the past decade, numerous works highlighted the anti-cancer and immunomodulatory properties of levan (Dong et al., 2015; Osman et al., 2023; Song et al., 2022; Xu et al., 2006).

Investigating the compatibility and effect of levan on the behavior of immune cells is crucial to pave the way for their biomedical application. For example, levan of *Bacillus subtilis* natto stimulates the production of cytokines and immunoglobulin E induced by ovalbumin via TLR4 in vitro and modulates the associated Th2 cell response in vivo (Xu et al., 2006). In addition, the murine macrophage cell line RAW264.7 produced nitric oxide, an M1 marker, when exposed to levan produced by the gram-negative soil bacterium *Tanticharoenia sakaeratensis* (Aramsangtienchai et al., 2020). Several works reported on the immunomodulatory properties of levans though only a limited number studied the underlying molecular mechanisms involved (Young et al., 2021). Recently, Young et al. demonstrated that the release of pro-inflammatory cytokines by immune cells upon exposure to bacterial levans stems from the presence of LPS contamination and not from an intrinsic immunomodulatory effect (Young et al., 2022). These results may jeopardize its potential application in this field and call for cleaner production processes. A wide range of microorganisms are used to produce levan-type fructans (Toksoy Öner et al., 2016). Due to advantages such as high yield and the ability to work under non-sterile conditions, the production of levans from halophilic bacteria such as *Halomonas* has gained interest (Kırtel et al., 2018; Kirtel et al., 2018). Especially, levan from *Halomonas smyrnensis* cultures (Erkorkmaz et al., 2022), namely *Halomonas* levan (HL), as well as its chemically modified derivatives have been extensively studied for various biomedical applications (Kirtel & Öner, 2021). *H. smyrnensis* mutants *co*-producing HL and poly(hydroxybutyrate) polyesters hold great industrial relevance (de Siqueira & Toksoy Öner, 2023), though fundamental bioactivity studies would require the use of HL enzymatically produced by the recombinant levansucrase enzyme to minimize adverse biological responses due to bacterial impurities. To the best of our knowledge, the interaction of *Halomonas* levans with macrophages has not been investigated before.

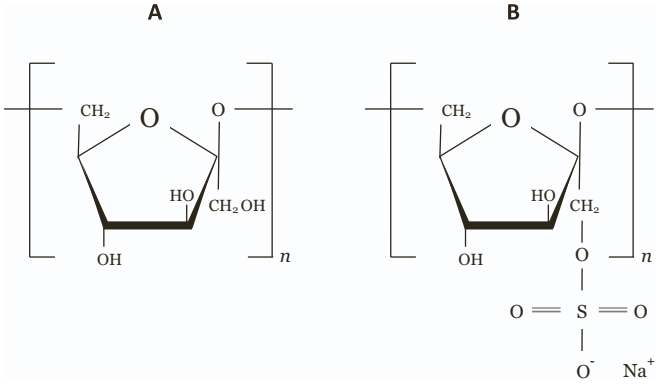

Scheme 1. Chemical structure of (A) levan and (B) sulfated levan.

Aiming to understand basic mechanisms associated with the activation of human macrophages by levans, in this work, we initially conducted compatibility studies of HL and hydrolyzed HL (hHL) and their sulfated derivatives (SHL and ShHL, respectively) (Scheme 1B) with the human monocyte-derived macrophage cell line THP-1. Then, we investigated their effects on the genotype and phenotype of M0 and M2 macrophages. Overall, our results indicate that these levans trigger an M1 polarization.

2. Experimental section

2.1. Production of Halomonas levan

HL was produced enzymatically in a two-step process. In the first step, the levansucrase enzyme from *H. smyrnensis* was expressed in recombinant *Escherichia coli* (*E. coli*) and purified. In the second, the enzyme was used for levan production in a sucrose containing reaction (Kirtel et al., 2018). Briefly, *E. coli* BL21 (DE3) cells harboring the pET28_sacB plasmid which contains the *sacB* levansucrase gene were grown in lysogenic broth (LB) medium in an orbital shaker at 37 °C and 180 rpm and then induced at the pre-stationary phase of their growth with isopropyl-β-D-thiogalactopyranoside (IPTG, neoFroxx, Einhausen, Germany). After overnight growth at 26 °C, cells were collected by centrifugation and lysed with sonication in the cell lysis buffer (20 mM phosphate buffer with 300 mM NaCl, pH 6.6). After centrifugation, the clarified cell lysate was passed through a Ni-NTA His-Bind Superflow affinity column (IMAC; Ni-NTA Superflow, QIAGEN, Hilden, Germany) and active fractions were collected. Then, the pure enzyme was added to the substrate solution containing 0.3 M sucrose and 3.5 M NaCl and left overnight at 15 °C to allow the synthesis of levan. The polymer in the reaction mixture was recovered by precipitation with absolute ethanol and dialyzed in cellulose membrane dialysis tubing with 14,000 Da of typical molecular weight cut-off (Sigma-Aldrich, St. Louis, MO, USA) against water for several days. Finally, the aqueous levan solution was purified by ion exchange chromatography in a Sepharose 6B weak ion column (Sigma-Aldrich) to remove charged impurities. The product was obtained after air-drying at 55 °C in a vacuum oven (Wisd Precise Vacuum oven OV-30, witeg Labortechnik GmbH, Wertheim, Germany).

To produce hHL, the product was hydrolyzed by microwave-assisted acid hydrolysis (Avsar et al., 2018). For this, levan was dissolved in acetic acid (5 % *w/v*) and the solution was irradiated in a house-hold microwave oven (Vestel MW GD-23, Manisa, Turkey) operated at 60 % of the maximum power (700 W), for up to 3 min. Cold absolute ethanol was added to the microwave-irradiated levan solution, the precipitate was stored at −20 °C overnight to enable the precipitation of hHL, the dispersion centrifuged at 8000 rpm for 30 min (Hermle/Z36HK, Gosheim, Germany) and the levan precipitate collected and dried in a vacuum oven (Wisd Precise Vacuum oven OV-30). The molecular weight distribution of hHL was determined by gel permeation chromatography (GPC) in a Tosoh EcoSEC HLC-8320-RI-UV GPC (Tosoh Bioscience, Tokyo, Japan) equipped with HQ-806 M and HQ-807 M columns and WYATT HELEOS-II MALS DynaPro DLS detector (Wyatt Technology Corp., Goleta, CA, USA). The molecular weights of HL and hHL were 51.30 ± 0.13 × 10^3 and 140.4 ± 69.4 kg/mol, respectively.

To synthesize sulfated derivatives, 2 % w/v HL and hHL dispersions were prepared in pyridine (Merck, Darmstadt, Germany) under magnetic stirring for 48 h at room temperature (RT), chlorosulfonic acid (Acros Organics B.V.B.A., Geel, Belgium) was added dropwise up to 1.5 mL per gram of levan and the reaction mixture was allowed to react under constant magnetic stirring for 12 h at RT (Avsar et al., 2018; Erginer et al., 2016; Gomes et al., 2018; Mihailescu et al., 2019). The reaction was stopped by the addition of a saturated Na_2CO_3 (Merck) solution in water. After phase separation occurs, the upper organic

phase was discarded and the aqueous phase containing SHL or ShHL was profusely dialyzed against water for several days and freeze-dried (Lyovac GT2, Steris Corp., Mentor, OH, USA). Sulfation degree (SD) of SHL and ShHL was analyzed following Erginer et al. (2016) and found to be 3.60 and 2.25, respectively. The molecular weight of SHL and ShHL was similar to the non-sulfated counterparts.

The structural integrity of HL and hHL was verified by heteronuclear single quantum correlation (HSQC) nuclear magnetic resonance (NMR) and Fourier-transform infrared spectroscopy (FT-IR). HSQC NMR characterization of levan samples (HL, hHL and ShHL) in D_2O solutions (Sigma-Aldrich) was conducted in at 600.13 MHz on a Bruker Avance III-600 spectrometer (Bruker BioSpin AG, Fällanden, Switzerland) equipped with a TCI Cryo ProbeTM fitted with a gradient along the *Z*-axis, at 27 °C. Spectra revealed the ^{13}C NMR peaks (ppm): C1(59.8), C6 (63.3), C4(75.0), C3(76.2), C5(80.2) and C2(104) and their corresponding ^{1}H NMR peaks (ppm): H1(3.54), H6(3.76), H4(3.96), H3(4.05) and H5(3.81) that are characteristic peaks of native levan (Fig. S1A). New broad ^{1}H NMR peaks between 4.1 ppm and 4.4 ppm corresponding to the ^{13}C NMR peaks between 66 and 70 ppm indicated the sulfation of the polysaccharide. These spectroscopic results were considered as solid evidence of successful levan sulfation. Characterization of the functional groups and bonding interactions of the HL, hHL, and ShHL were performed by FT-IR spectroscopy (Jasco FT/IR-4700, Tokyo, Japan) analysis. The measurements were recorded at the mid-IR region from 4000 to 400 cm^{-1} at 4 cm^{-1} resolution under ambient temperature (25 °C). The characteristic absorption band of the –OH stretching of fructofuranose rings around 3300 cm^{-1}, C—H stretching vibration of fructose residues around 2930 cm^{-1} and the three characteristic C–O–C bands at around 1415, 1010 and 920 cm^{-1} typical for levan polysaccharide were all detected. For the ShHL sample, the new bands of FTIR analysis showed the new bands at 1215 cm^{-1} (S=O) and 797 cm^{-1} (C–O–S) of the C–O–SO_3 groups were also shown (Fig. S1B).

2.2. Cell compatibility of levan derivatives

The cell compatibility of HL, SHL, hHL and ShHL was assessed in the human monocyte THP-1 cell line (ATCC® TIB-202™, American Type Culture Collection, Manassas, VA, USA) that was generously donated by Prof. David (Dedi) Meiri (Faculty of Biology, Technion – Israel Institute of Technology) and cultured in RPMI-1640 (Life Technologies Corp., Carlsbad, CA, USA) supplemented with L-glutamine, 10 % heat-inactivated fetal bovine serum (FBS, Sigma-Aldrich) and a 1 % penicillin/streptomycin antibiotic mixture (5 mL of a commercial mixture of 100 U/mL penicillin +100 μg/mL streptomycin per 500 mL medium, Sigma-Aldrich) and incubated at 37 °C in humidified, 5 % CO_2 atmosphere. Cells were split every 3–4 days.

To assess the compatibility of different levan derivatives, THP-1 monocytes were initially differentiated into macrophages. For this, cells were grown in 96-well plates (20×10^3 cells/well) and phorbol 12-myristate 13-acetate (50 ng/mL, PMA, Sigma-Aldrich) was added for 24 h in a serum-free-RPMI-1640 medium and allowed to attach to the surface at 37 °C and 5 % CO_2. Then, cells were washed twice with phosphate buffer saline (PBS, pH 7.4, Sigma-Aldrich) and the medium was replaced by RPMI-1640 containing 10 % FBS. After resting for 24 h, different volumes of levan stock solutions (1 % *w/v* in PBS) were added to obtain final levan concentrations of 0.01 %–0.5 % w/v. For these assays, stock levan solutions (1 % *w/v*) in PBS were sterilized by filtration (sterile 0.22 μm syringe filters, Merck Millipore Ltd., Cork, Ireland) under a biological hood. After 24, 48 and 72 h incubation, the medium was removed, and new medium (100 μL) and sterile 3-(4,5 dimethylthiazol-2-yl)-2,5-diphenyltetrazolium bromide (MTT, 25 μL, 5 mg/mL, Sigma-Aldrich) was added. After 2 h incubation at 37 °C and 5 % CO_2, formazan crystals were dissolved in 100 μL of dimethyl sulfoxide (DMSO, Sigma-Aldrich) and the absorbance was measured at 530 nm (with reference to the absorbance at 670 nm) in a spectrophotometer (Multiskan GO™, Thermo Fisher Scientific Oy, Vantaa, Finland). Cells treated only with culture medium (control) were considered as 100 % viable.

2.3. THP-1 cell total RNA-sequencing

To test the effect of hHL and ShHL on THP-1 gene expression, we carried out RNA-sequencing (RNA-seq) analysis. For this, THP-1-derived macrophages were grown in 6-well plates (1.5×10^6 cells/well) with 1.5 mL of RPMI-1640 medium containing sterile levan solutions (0.1 % w/v in PBS) or without levan (control). Cells were incubated for 24 h at 37 °C. All experiments were performed in triplicate or quadruplicate ($n = 3$ or 4 for each experimental group). Then, the cell medium was removed, and wells were washed with PBS and 700 μL of TRIzol (Invitrogen, Carlsbad, CA, USA) was added. The RNA was extracted according to a standard protocol and stored at −80 °C until further use. RNA was sequenced by CEL-seq, using Illumina HiSeq 2500 (Illumina, Inc., San Diego, CA, USA) at the Technion Genome Center. FASTQC (version 0.11.5, Babraham Bioinformatics, The Babraham Institute, Cambridge, UK) was used for quality control and the reads were mapped by Tophat2 version 2.1.0 algorithm (Trapnell et al., 2012) to genome assembly. HTseq-count version 0.11.2 (Campbell et al., 2013) was used to count the reads, and the normalization of raw counts and differential expression were calculated using DESeq2 in R platform version 1.24.0 (Love et al., 2014), with Padj using Benjamini and Hochberg correction for false discovery.

2.4. Bioinformatics analysis of RNA-seq data

A principal component analysis (PCA) plot was generated by a plot that spans the samples in 2D plane by their first two principal components using DESEQ2 package in R platform (Love et al., 2014). Gene ontology (GO)-biological process pathway enrichment analysis of the differentially expressed genes (DEG) was generated based on the top-20 significantly upregulated protein-coding-genes for each treatment using ShinyGO v0.76 webserver (Xijin Ge et al., 2020), with the following settings: (i) search for species was human, (ii) false discovery rate (FDR) was 0.05, and (iii) pathway database was GO biological process. *P-value* for enrichment analysis was calculated via hypergeometric distribution, followed by correction for multiple comparisons using FDR. The Kyoto Encyclopedia of Genes and Genomes (KEGG) database is a collection of biological pathways, disease pathways, and functional modules, which provide a comprehensive understanding of cellular and organismal functions. GSEA is a widely used tool for assessing pathway enrichment in transcriptional data. In this approach, all genes in the RNA-seq data could be ranked based on their fragments per kilobase of exon per million (FPKM) values, and GSEA could be applied using version 4.3.2 of the GSEA software (http://www.gsea-msigdb.org/gsea/login.jsp; version 4.3.2) (Subramanian et al., 2005). In this study, we investigated the Hallmarks (h.all.v2022.1.Hs.symbols.gmt) and c2.KEGG (c2.cp.kegg.v2022.1.Hs.symbols.gmt) gene set collections from the Molecular Signature Database (MSigDB) (Liberzon et al., 2011, 2015). The Array Annotations database (Human_Ensembl_Gene_ID_MSigDB.v2022.1.Hs.chip) from the MSigDB collection was utilized to convert Ensemble IDs to gene symbols for all genes. To determine statistically significant enriched pathways, a cutoff value of FDR < 0.25 and normal $P < 0.05$ was applied.

2.5. THP-1 cell real time-quantitative polymerase chain reaction

To check the expression of specific genes, we conducted real time-quantitative polymerase chain reaction (RT-qPCR) analysis. For this, THP-1-derived macrophages were grown in 24-well plates (2×10^5 cells/well) in 6-well plates (1.5×10^6 cells/well) in 1.5 mL of RPMI-1640 medium. After resting for 24 h, cells were exposed to two different treatments: (i) sterile hHL and ShHL solutions (0.1 % *w/v*) for 24 h, (ii) pretreatment with IL-4 (20 ng/mL, Biolegend, San Diego, CA,

USA) for 24 h and incubation with sterile hHL and ShHL solutions (0.1 % *w/v*) for 24 h. Untreated cells were used as control. Sample quality was assessed by a spectrophotometer (NanoDrop Technologies, Wilmington, DE, USA). The 260/280 ratios in all the samples were > 1.8, and the 260/230 ratios were > 1.7. cDNA was synthesized from 1 μg of RNA with the qScript™ cDNA synthesis kit (Quanta Biosciences, Gaithersburg, MD, USA) according to the manufacturer's instructions. The mRNA expression levels of human *IL-6* (Hs00174131_m1), *C-X-C Motif Chemokine Ligand 8* (*CXCL8*, Hs00174103_m1) and *β-actin* (Hs99999148_m1) were quantified using TaqMan® Gene Expression assays (Applied Biosystems, Thermo Fisher Scientific, Waltham, MA, USA) and a QuantStudio1 RT-qPCR instrument (Applied Biosystems, Waltham, MA, USA). The relative quantity (RQ) values were calculated according to the $2^{-\Delta\Delta Ct}$ method, which reflects the differences in the threshold for each target gene relative to β-actin and untreated-control cells.

2.6. THP-1 cell cytokine release

THP-1-derived macrophages were exposed to hHL and ShHL solutions and the concentrations of IL-6, IL-1β, IFN-γ, IL-8, IL-10, IL-4 and IL-17A were quantified using commercial enzyme-linked immunosorbent assays (ELISA) kits supplied by Biolegend and the concentration of tumor necrosis factor alpha (TNF-α) was determined using a commercial ELISA kit (Invitrogen). For this, THP-1-derived macrophages were grown in 24-well plates (2×10^5 cells/well) in 500 μL of RPMI-1640 medium. After resting for 24 h, cells were exposed to two different treatments: (i) sterile hHL and ShHL solutions (0.1 % *w/v*) for 24 h, (ii) pretreatment with IL-4 (20 ng/mL, Biolegend) for 24 h and incubation with sterile hHL and ShHL solutions (0.1 % w/v) for 24 h. Untreated cells were used as control. Following the treatment, the medium was replaced by fresh medium that was collected after 72 h, centrifuged to remove cell debris, and kept in −80 °C until analysis. Finally, the concentration of the different cytokines was quantified using ELISA kits according to the manufacturer's instructions. The absorbance was measured at 450 nm (with reference to the absorbance at 570 nm) using a Spectrophotometer (Multiskan GO™).

2.7. Statistical analysis

All statistical analyses were conducted by using GraphPad Prism software version 7.04 (GraphPad Software, San Diego, CA, USA). Results are reported as the mean ± S.D. of at least three independent experiments. A value of at least $P \leq 0.05$ was considered significant for all tests. We used the DESeq2 R package (www.bioconductor.org) to conduct differential expression analysis, which involves generating a normalized count matrix and performing statistical tests to detect differences in gene expression between samples. Specifically, we employed the Wald hypothesis test offered by DESeq2 for our analysis.

3. Results and discussion

3.1. Cell compatibility of levan derivatives

Macrophages are a type of white blood cell that recognizes and eliminate foreign invaders, such as bacteria, viruses, and debris (Barron & Wynn, 2011; Correa-Gallegos et al., 2021). They act as a first line of defense against infection and play a crucial role in the innate immune response (Jung et al., 2020). Different macrophage cell lines have been used as a model of macrophage polarization in vitro. The human THP-1 (Genin et al., 2015) cell lines is among the most widely used. In addition, it was recently reported that THP-1 monocytes differentiated with PMA and primary human macrophages share similarities in key transcriptional programs associated with the polarization (Li et al., 2021). A critical stage before characterizing the effect of levan derivatives on the macrophage phenotype to ensure that they do not cause cell death >30 %, as established by the ISO 10993-5 guidelines (*International Organization for Standardization, ISO 10993-5:2009 Biological Evaluation of Medical Devices Part 5: Tests for* in Vitro *Cytotoxicity.*, n.d.). In this context, the viability of the macrophage cell line exposed to different levan concentrations (0.01–0.5 % *w/v*) for 24, 48 and 72 h was estimated by the MTT assay. In general, all non-hydrolyzed and hydrolyzed levan samples showed high macrophage compatibility at all the tested concentrations and incubation times (Fig. 1). In addition, no morphological changes were observed upon exposure of these cells to the different levans (data not shown). Cytocompatibility of microbially produced HL and its derivatives have been reported for numerous cell lines like fibroblasts, osteoblasts, myoblasts, keratinocytes, and various adenocarcinoma cells in our previous studies (Kirtel & Öner, 2021). Also recently, resveratrol loaded enzymatically produced hHL nanoparticles were found to improve cellular viability of dermal fibroblasts (Cinan et al., 2021). Hydrolyzed levan derivatives offer several advantages for use in the pharmaceutical industry, including increased solubility and lower viscosity, and disruption of the self-assembled spheroidal structures, as demonstrated by dynamic light scattering data (data not shown), and hence improved control over synthesizing functional biomaterials. In fact, when lipid nanoparticles were coated with quaternized hHL, the burst release of paclitaxel was prevented for 6 h (Mutlu et al., 2021). Also, immunomodulatory studies on plant systems showed improved pathogen resistance with hHL rather than HL in *Arabidopsis thaliana* (Janse van Rensburg et al., 2020) and chicory (*Cichorium intybus*) (Versluys et al., 2022). Based on these results, in advance, the genotypic and phenotypic changes on macrophages were assessed with hHL and ShHL. It is worth mentioning that the immunomodulatory activity of levan changes with the molecular weight (Aramsangtienchai et al., 2023).

3.2. Modulation of the genotype of human macrophages by levan derivatives in vitro

Macrophages possess remarkable plasticity and can undergo diverse functional transformations depending on microenvironmental stimuli (Locati et al., 2020). M1 macrophages produce pro-inflammatory cytokines (e.g., TNF-α, IL-6, IL-8 and IL-1β), while M2 ones produce anti-inflammatory cytokines (e.g., IL-10, IL-4, and IL-17A) (Liu et al., 2021; Yunna et al., 2020). Polysaccharides have been shown to trigger macrophage polarization (Li et al., 2022; Wang et al., 2022; Wei et al., 2019). M1 macrophages often express higher levels of tissue necrosis factor (*TNF*) and C—C motif chemokine ligand (*CCL*) gene families, while M2 macrophages highly express other genes, such as of cluster of differentiation 163 (*CD163*) and mannose receptor C-type 1 (*MRC1*) genes (Kumar, 2019; Locati et al., 2020). Initially, M0 (untreated) THP-1 cells were incubated for 24 h with hHL or ShHL (0.1 % w/v) and the expression levels of the whole genome were quantified by RNA-seq. Following RNA-seq data collection, a total of 27,726 transcripts were detected. PCA of the 50 top variable genes showed a prominent separation between control macrophages and those exposed to hHL or ShHL treatments. PCA of the top 10,000 variable genes also indicates a good separation between the treatment groups to the control group, and the start of integrating of the two different treatments is observed (Fig. 2A). These results clearly indicate that both hHL and ShHL treatments for 24 h affect THP-1 macrophage gene expression. After filtering the DEG data by $P \leq 0.05$, a set of 923 transcripts remained for the hHL treatment (338 were upregulated and 585 downregulated) and a set of 772 transcripts remained for the ShHL treatment (367 were upregulated and 405 downregulated). In addition, 185 and 230 genes were upregulated and downregulated for both treatments, respectively. Among the 15-top upregulated genes, we identified six genes belonging to the *CCL* gene family (*CCL2*, *CCL3*, *CCL3L1*, *CCL4* and *CCL20*) and two genes (*CXCL3* and *CXCL8*) belonging to the *CXC* gene family (Fig. 2B), which are known to control the differentiation, activation, and migration of immune cells (Vyshkina et al., 2008). M1 macrophages typically highly

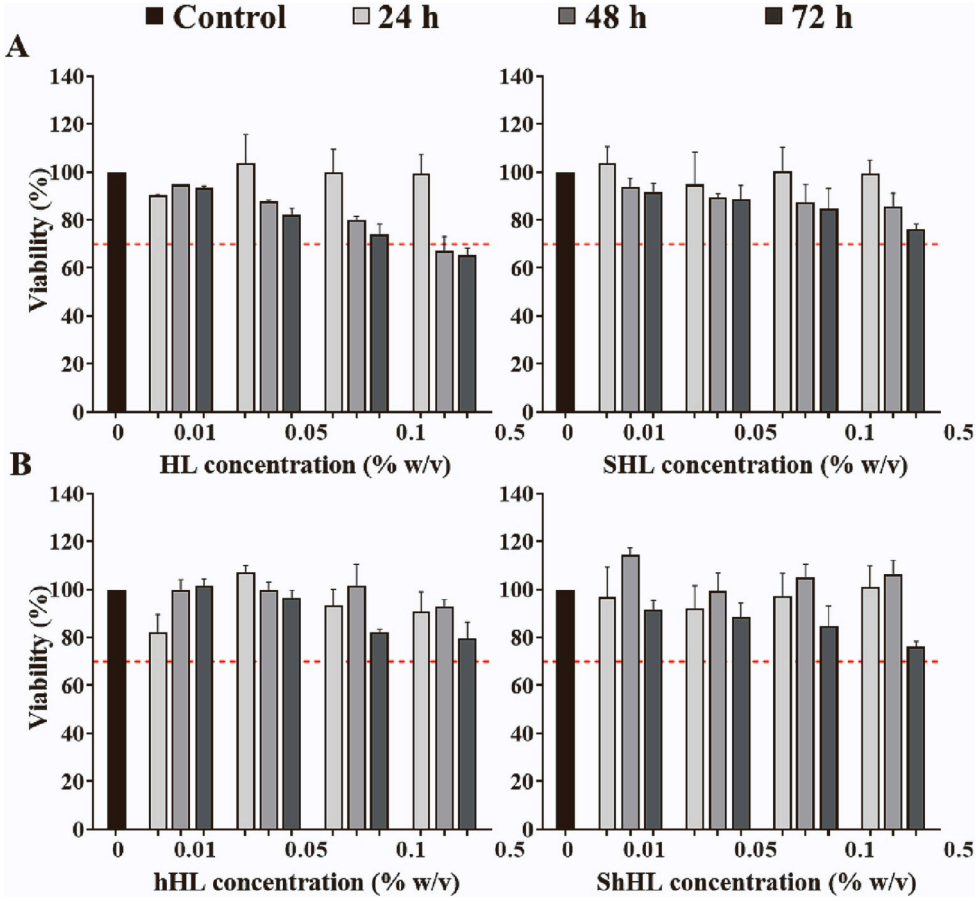

Fig. 1. THP-1 cell viability upon incubation with levan derivatives (0.01–0.5 % *w/v*) for 24–72 h at 37 °C, as determined by the MTT assay. (A) THP-1 cells treated with non-hydrolyzed levan derivatives and (B) THP-1 cells treated with hydrolyzed levan derivatives. Results are expressed as mean ± S.D. of at list three independent experiments ($n = 3$).

express *CXC* genes (Wang, Smith, et al., 2019). Our data point out that THP-1-derived macrophages exposed to levans express higher levels of various genes related to a pro-inflammatory response than untreated controls. For example, cells exposed to hHL and ShHL showed 3.5- and 7.2-fold change (FC) of *CCL4*, respectively, when compared to controls (Fig. 2B). A similar trend was observed for *CXCL8* (3.0 and 5.2 FC for hHL and ShHL, respectively) and *TNF* (2.6 and 3.8 FC for hHL and ShHL, respectively) (Fig. 2B). The *CCL4* gene encodes for a pro-inflammatory CCL4 chemokine, also known as macrophage inflammatory protein-1 beta (MIP-1β) (Gakharia et al., 2022). *CXCL8* gene encodes for a pro-inflammatory IL-8 and is generally considered to be pro-inflammatory, as it promotes the recruitment and activation of neutrophils at sites of inflammation (Campbell et al., 2013; Koper-Lenkiewicz et al., 2022). *TNF-α*, among others, has been shown to play a key role in the cytokine cascade in many inflammatory conditions (Liu et al., 2021).

Several important pathways associated with immune response were identified in the GO-biological process enrichment analysis of the 20-top significantly upregulated genes in the RNA-seq data as a response to hHL or ShHL treatments (Table S1). Among them, chemotaxis of different cells (as a response to hHL treatment), response to chemokines and inflammatory response (as a response to ShHL treatment) (Fig. 3A,B). Moreover, when conducting GO-biological process enrichment analysis on all the significantly upregulated genes in both hHL and ShHL treatments (Table S2), various immune-related pathways were indicated. One of these pathways was cellular response to LPS (Fig. S2).

To gain insight into the mechanisms and pathways involved in the hHL and ShHL effect on THP-1-derived macrophages, GSEA was conducted with RNA-seq datasets, with FDR < 0.25 as the cut-off value. Since GSEA does not rely on a gene list of interest but on the entire ranking of genes, it has been shown to provide greater sensitivity to find gene expression changes of small magnitude that operate coordinately in specific sets of functionally related genes. GSEA calculates separate enrichment scores for each pairing of a sample and normalizes it to the number of genes in the gene set to get the normalized enrichment scores (NES) (Subramanian et al., 2005).

Signaling of TNF-α via nuclear factor kappa-light-chain-enhancer of activated B cells (NfKb) has long been considered a prototypical pro-inflammatory signaling pathway, as it is mainly based on the activation by pro-inflammatory cytokines (Koper-Lenkiewicz et al., 2022). IL-6/Janus kinase/Signal transducer and activator of transcription 3 (IL-6/JAK/STAT3) signaling is a critical pathway involved in the pro-inflammatory response and is activated in response to various stimuli such as infection, tissue damage, and stress (Wu et al., 2021). Reactive oxygen species (ROS) are involved in the activation of pro-inflammatory transcription factors that promote the expression of pro-inflammatory cytokines which play key roles in the initiation of the inflammatory response (Herb et al., 2019; Naik & Dixit, 2011; Rendra et al., 2019). GSEA results of the hHL treatment revealed that the most significantly enriched gene set corresponded to genes with increased expression in TNF-α-signaling via NfKb (NES = 1.59) (Fig. 3C). Many other gene sets focused on immune-related pathways, such as IFN-γ response (NES = 1.2), though with an FDR value above 0.25. GSEA results of the ShHL treatment revealed that most gene sets focused on immune-related pathways. The most significantly enriched gene set corresponded to genes with increased expression in TNF-α-signaling via NfKb (NES = 2.11), majority of the genes were enriched for inflammatory response (NES = 1.82), IL-6/JAK/STAT3 signaling, (NES = 1.57), oxidative phosphorylation (NES = 1.43) and ROS pathway (NES = 1.29) (Fig. 3C).

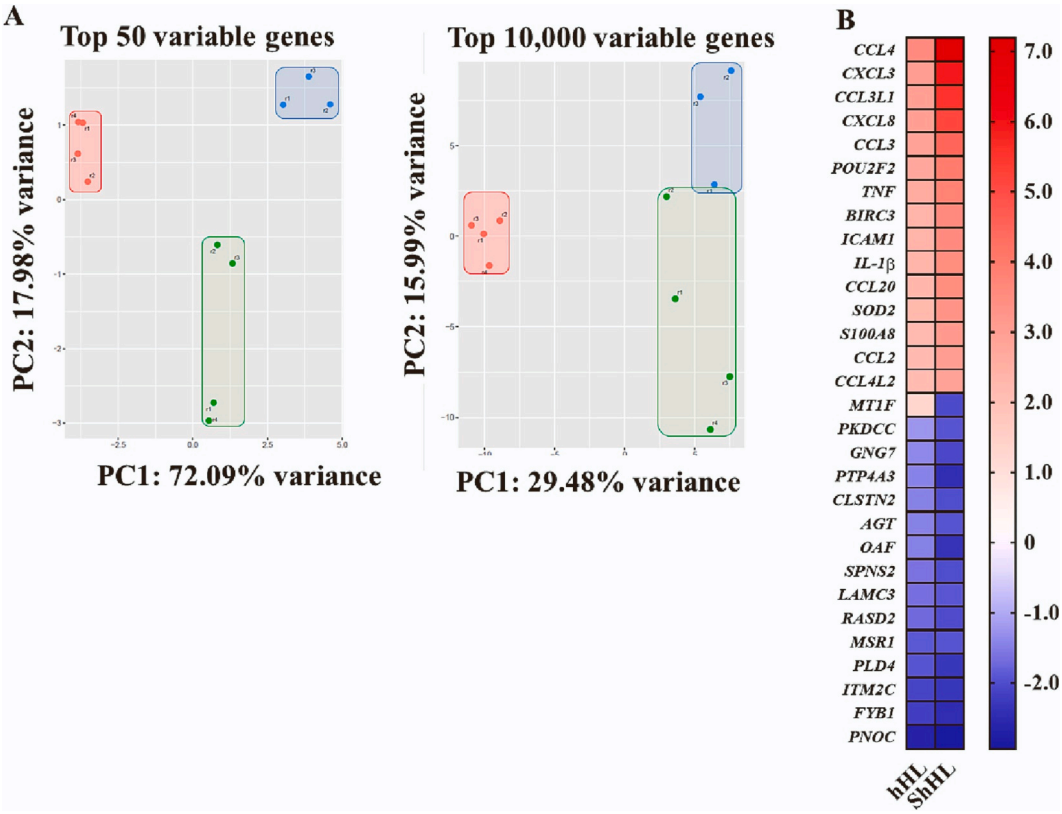

Fig. 2. PCA plot and heatmap of macrophage transcriptomes. (A) PCA plot of RNA-seq data of the top 50 or 10,000 variable genes. Control (red), ShHL (blue) and hHL (green). (B) RNA levels of the 15 top upregulated and 15 top downregulated genes, based on RNA-seq of THP-1-derived macrophages after 24 h of treatment with either hHL or ShHL. The data for each gene are shown as fold change (FC) relative to its mean level.

To gain a deeper understanding of the molecular mechanisms underlying the experimental results and to provide insights into potential therapeutic applications of levan derivatives, we conducted KEGG analysis which is used to classify DEG by biological pathways. Among the enriched KEGG pathways, we identified cytokine-cytokine receptor interaction, Toll-like receptor signaling pathway and chemokine signaling pathway, all with FDR < 0.25 (Table S3). Taken together, RNA-seq results strongly suggest that treatment with either hHL or ShHL stimulates a pro-inflammatory immune response in THP-1-derived macrophages, as GSEA studies indicate high correlation with pro-inflammatory signaling pathways.

To validate the observed alterations in the gene expression, we conducted RT-qPCR analysis to evaluate the effects of hHL and ShHL treatments. Following a 24-h incubation of M0 (THP-1-derived macrophages) or IL-4-polarized M2 macrophages with hHL or ShHL (0.1 % *w/v*), we quantified the mRNA expression levels of *IL-6* and *CXCL8*. Both *IL-6* and *CXCL8* genes encode for pro-inflammatory pathways (Campbell et al., 2013). The data indicated that treatment of non-polarized macrophages with hHL or ShHL resulted in a marked up-regulation of IL-6 expression levels by 6.1-fold and 39.8-fold, respectively, though differences were not statistically significant (Fig. 4A). Additionally, treatment with hHL or ShHL induced the upregulation of *CXCL8* expression levels in non-polarized macrophages, with a statistically significant fold increase of 25.4 and 16.6, respectively ($P = 0.03$) (Fig. 4A). Moreover, pre-treatment of IL-4-polarized macrophages (to polarize them into M2) with hHL or ShHL resulted in a statistically insignificant increase of the expression levels of *IL-6* by 3.5- and 3.7-fold, and a statistically significant increase of *CXCL8* by 12.3- and 7.4-fold (Fig. 4B). All in all, our findings indicate that these levans elicits a robust pro-inflammatory reaction and has the potential to reprogram IL-4-polarized M2 macrophages to M1 phenotype, as evidenced by the upregulation of *IL-6* and *CXCL8* expression levels following treatment.

M1 macrophages are characterized by a high capacity to present antigen, as well as high pro-inflammatory cytokine production (IL-6 and IL-1β, IFN-γ, IL-8) (Arabpour et al., 2021; Wang, Smith, et al., 2019), while M2 are characterized by the release of anti-inflammatory cytokines, and exhibit diverse phenotypic and functional subpopulations (M2a, M2b, M2c, M2d) according to the induced molecules and transcription products. For example, M2a macrophages induced by exposure to IL-4 and IL-13 play a key role in the wound-healing process. They also secrete various cytokines, including IL-10 and TGF-β. M2b macrophages, also known as regulatory macrophages, secret pro-inflammatory cytokines, such as IL-1β, IL-6, and TNF-α, and significant amounts of the anti-inflammatory cytokine IL-10 and low levels of IL-12 (Wang, Smith, et al., 2019). The M2c subtype exhibits anti-inflammatory activity by the release of substantial amounts of IL-10 and transforming growth factor-beta (TGF-β). M2d macrophages, also known as tumor-associated macrophages, mainly characterized by high IL-10, TGF-β, and low IL-1β production (Feng et al., 2021; Nakai, 2021; Wang, Smith, et al., 2019).

Based on our previous results, which indicate a pro-inflammatory response when THP-1 macrophages are exposed to these levan derivatives, and to gain deeper understanding on the activation state of these macrophages, we quantified the release of IL-6, IL-1β, IFN-γ, TNF-α, IL-8, IL-10, IL-4 and IL-17A cytokines by unpolarized-resting THP-1-dervied macrophages (M0) and by IL-4-polarized macrophages, 72 h after treatment with hHL or ShH (0.1 % *w/v*). It can be noticed that secretion of the pro-inflammatory cytokine IL-6 was significantly ($P <$ 0.0001) higher when M0 cells were exposed to ShHL with respect to untreated counterparts (Fig. 5A). These results are in good agreement with the GSEA results which showed a gene enrichment in the IL-6/JAK/STAT3 signaling pathway and the RT-qPCR data, which showed elevated levels of *IL-6* mRNA expression in unpolarized-resting macrophages treated with ShHL. Furthermore, IL-4-polarized macrophages, known for their anti-inflammatory phenotype, exhibited minimal IL-6

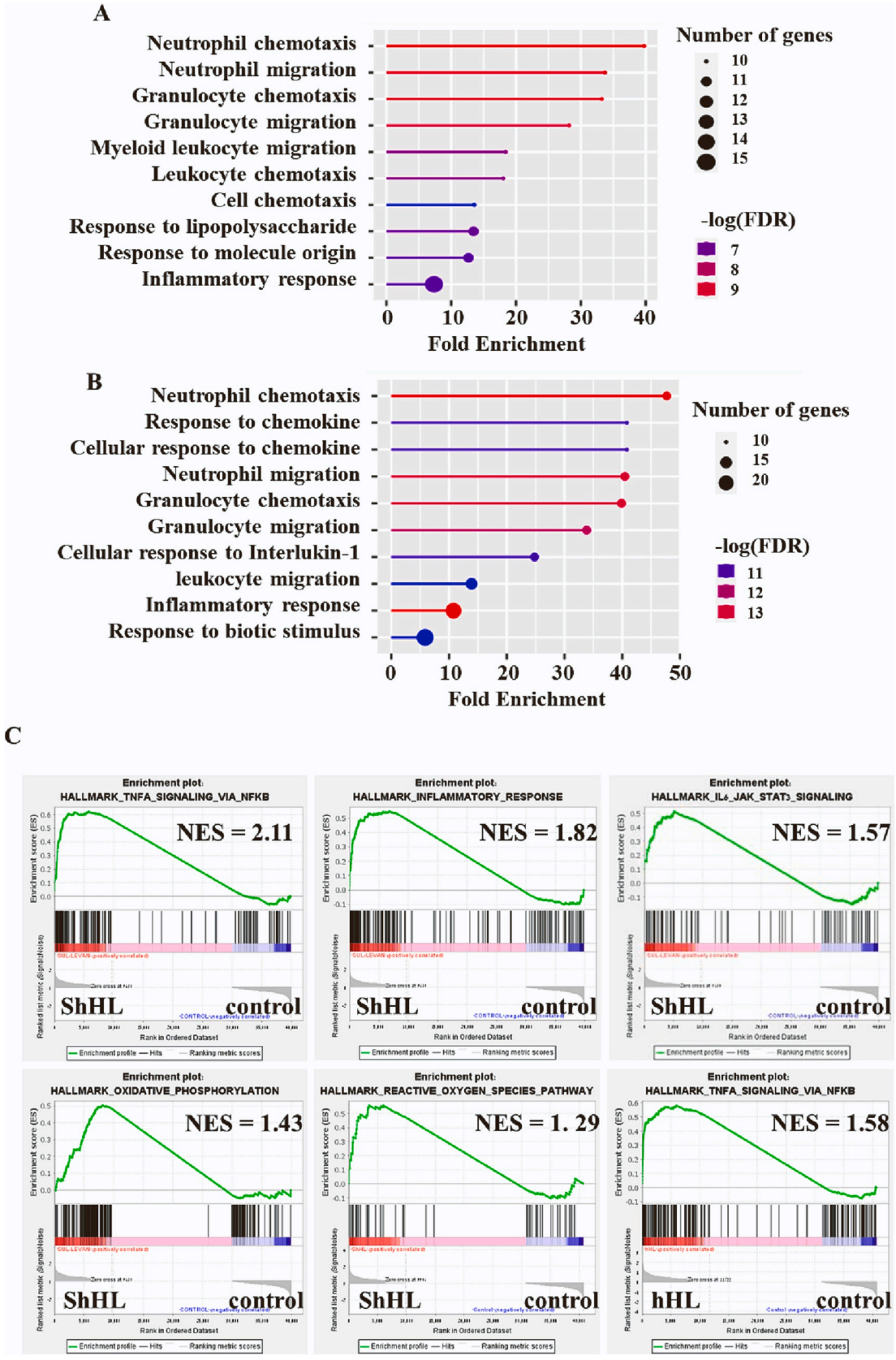

Fig. 3. GO enrichment analysis and GSEA. (A) GO enrichment analysis of 20-top significantly upregulated genes found in RNA-seq data after 24 h of treatment with hHL and (B) ShHL in THP-1-derived macrophages. (C) GSEA enrichment plots of the correlation of ShHL treatment with TNA-α- signaling via NfKb, inflammatory response, IL-6/JAK/STAT3 signaling, oxidative phosphorylation, oxidative phosphorylation and ROS pathway, and the correlation of hHL treatment with TNA-α-signaling via NfKb, NES value is applied in each plot.

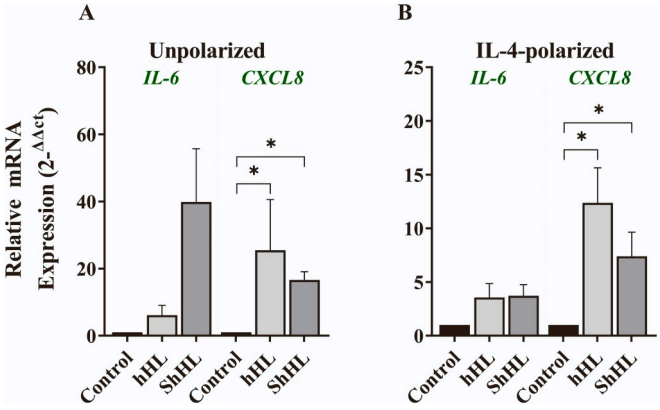

Fig. 4. RT-qPCR of (A) M0 (unpolarized) or (B) IL-4-polarized macrophages cultured with 0.1 % w/v hHL and ShHL for 24 h. Total RNA was isolated from macrophages and then reverse transcribed into cDNA. RT-qPCR was conducted to determine the number of copies of cDNA for each gene, and relative mRNA expression levels were calculated for each gene and normalization against β-actin, using RQ (relative quotient), as determined by $2^{-\Delta\Delta Ct}$ method. Statistical analysis was conducted using one-way ANOVA, followed by Tukey correction with GraphPad Prism 8.0.1. Mean ± S.D. ($n = 3$ or 4). Statistically significant difference between values (* $P < 0.05$).

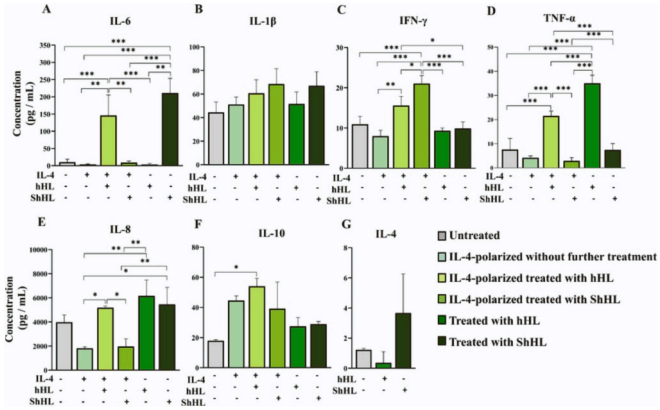

Fig. 5. Cytokine release of THP-1-derived macrophages. The cytokine concentrations (pg/mL) of (A) IL-6, (B) IL-1*β*, (C) IFN-γ, (D) TNF-α, (E) IL-8, (F) IL-10 and (G) IL-4 was measured using supernatants of M0 (untreated) or IL-4-polarized macrophages cultured with 0.1 % *w/v* hHL and ShH for 24 h. Statistical analysis was conducted using one-way ANOVA, followed by Tukey correction, using GraphPad Prism 8.0.1. Mean ± S.D. ($n = 3$ or 4). Statistically significant difference between values (* $P < 0.05$; ** $P < 0.01$, *** $P < 0.001$).

secretion, while hHL treatment resulted in enhanced secretion of IL-6, as compared to cells treated with IL-4 alone. In contrast, ShHL treatment had no significant effect on IL-6 secretion by IL-4-polarized macrophages, which is consistent with the RT-qPCR data indicating higher *IL-6* mRNA expression levels in these cells upon ShHL treatment.

The RNA-seq data obtained from this study unveils a notable increase in the expression levels of *IL-1β* and *CXCL8* genes, which encode for the pro-inflammatory cytokines IL-1β and IL-8, respectively, upon treatment with either hHL or ShHL. Notably, while the secretion of IL-1β remained unchanged following treatment with these levan derivatives, a statistically significant ($P = 0.02$) increase in IL-8 release was observed upon treatment of IL-4-polarized macrophages with hHL (Fig. 5B,E). These results are in line with the RT-qPCR findings, which demonstrate a robust upregulation of *CXCL8* mRNA expression levels in response to hHL or ShHL treatment. Additionally, hHL treatment of IL-4-polarized macrophages resulted in a remarkable increase in the secretion of IL-8 compared to untreated cells (Fig. 5E). Consistent with this, the RT-qPCR data also revealed a significant increase in *CXCL8* expression in hHL-treated IL-4-polarized macrophages as compared to untreated cells.

As excepted, IL-4-polarized macrophages secreted lower amounts of pro-inflammatory IFN-γ compared to the unpolarized counterparts. Yet, in the presence of hHL or ShHL, IL-4-polarized macrophages secret significantly higher amounts ($P = 0.002$ and $P = 0.0001$, respectively) of IFN-γ (Fig. 5C). These results are good agreement with GSEA data that suggested gene enrichment of the IFN-γ response (NES = 1.2, FDR = 0.25) in the ShHL treatment.

GSEA results also revealed a gene enrichment in the TNF-α-signaling via NfKb pathway upon both hHL and ShHL treatments. Increase in the expression levels of the pro-inflammatory cytokine TNF-α has also been reported for long chained levan from *Bacillus licheniformis* (Susan Van Dyk et al., 2012), *Paenibacillus* sp. (Xu et al., 2016) and short chained *B. subtilis* levans (Magri et al., 2020) each accompanied with different cytokine expression profiles mainly attributed to their structural differences such as chain length and degree of branching (Young et al., 2021). Recently, Aramsangtienchai et al. showed that the molecular weight of levan affects its immunomodulatory activity in a murine macrophage cell line in vitro (Aramsangtienchai et al., 2023). Accordingly, TNF-α secretion was significantly ($P < 0.001$) higher when M0 cells were exposed to hHL. Nonetheless, in the presence of hHL, IL-4-polarized macrophages secrete significantly ($P < 0.001$) higher amounts of TNF-α. Despite it, TNF-α secretion did not change when the cells were treated with ShHL (Fig. 5D). The results presented here provide compelling evidence that the treatment of resting macrophages with levan derivatives elicits a robust pro-inflammatory cytokine response, indicating a shift towards an M1-like phenotype. Moreover, our findings suggest that treatment of IL-4-polarized macrophages with levan derivatives can effectively reprogram these cells towards an M1-like state. Interestingly, the release of the anti-inflammatory cytokine IL-10 was higher, although statistically insignificantly, upon exposure to either hHL or ShHL than in untreated cells. This result may stem from the complex interplay of various signaling pathways and transcription factors involved in macrophage polarization (Yunna et al., 2020). For instance, polysaccharides can activate different signaling pathways in macrophages, leading to the production of both pro-inflammatory and anti-inflammatory cytokines (Huang et al., 2019; Pu et al., 2019). For example, Baseler et al. reported that the LPS-driven IL-10 production functions as a metabolic rheostat in macrophages, enabling them to maintain metabolic equilibrium during M1 macrophage differentiation and they showed that stimulated macrophages can produce relatively high levels of IL-10 (Baseler et al., 2016). These findings suggest that this cytokine might participate in autocrine and paracrine control of metabolic programing and highlight the complexity of the analysis. As anticipated, secretion of the anti-inflammatory IL-10 cytokine was higher in IL-4-polarized cells than in untreated macrophages, and IL-10 secretion from IL-4-polarized macrophages treated with hHL (but not ShHL) was even higher (Fig. 5F). Likewise, non-significant changes were observed in IL-4 cytokine release, which was very low in all cases and under the standard range (Fig. 5G). Finally, IL-17A cytokine concentrations were under detection level (data not shown).

Collectively, the results are very consistent with the GSEA and RT-qPCR data. Notably, following exposure to hHL or ShHL, macrophages demonstrated a marked and significant upregulation in the secretion of pro-inflammatory cytokines. hHL induced the secretion of TNF-α and IL-8, while ShHL increased the secretion of IL-6 and IL-8, highlighting the contrasting effects of the two derivatives on THP-1-derived macrophages. Moreover, treatment with hHL reprogrammed IL-4-polarized (M2) macrophages to the M1 state, as evidenced by the increased release of pro-inflammatory cytokines, including IL-6, IFN-γ, TNF-α and IL-8.

Sulfated polysaccharides, namely glycosaminoglycans, are main components of the extracellular matrix and cell surface and are known to play key roles in many biological processes due to their interactions with growth factors, chemokines, cytokines, adhesion molecules,

enzymes, etc. Glycomimetics has been a very efficient strategy to obtain smart materials with tunable properties (Tamburrini et al., 2020) and hence considerable amount of research has been devoted to synthesizing sulfated derivatives with desired functionalities. Also in our research, sulfated levan derivatives have been shown to have heparin mimicry through thrombin inhibition (Erginer et al., 2016), to improve not only the cytocompatibility and myoconductivity of multilayered free-standing membranes (Gomes et al., 2018) but also the antithrombogenic activity of electrospun nanofibrous membranes (Avsar et al., 2018) and laser deposited multifunctional coatings (Mihailescu et al., 2019). According to our results, hHL and ShHL have a differential impact on the inflammatory response of human macrophages in vitro, as expressed by changes in cytokine secretion. These differences most probably stem from their physicochemical properties which can influence their interaction with macrophages and intracellular signaling pathways. Sulfation introduces negative charges to the polysaccharide backbone, which can affect its interaction with the negatively-charged cell membrane and reduce binding due to electrostatic repulsion. This change in the polysaccharide-macrophage interaction most likely leads to changes in macrophage activation with respect to non-sulfated derivatives.

4. Conclusions

Extensive research has been conducted to understand the effect of different polysaccharides on the activation of macrophages. Despite its potential as an immunostimulant, the mechanisms by which levan-type frucatns interact with immune cells have not been fully elucidated. In this work, we initially investigated the cell compatibility of four structurally different *Halomonas* levan polymers, namely HL, hHL, SHL and ShHL on human macrophages and all forms were compatible with these cells at concentrations of up to 0.5 % w/v. Then, we studied the effect of hHL and ShHL on the polarization of the human macrophage cell line THP-1 at the gene and cytokine levels. GSEA and KEGG analysis of the RNA-seq data provided insight into the effect of hHL and ShHL on human THP-1-derived macrophages, demonstrating that both derivatives stimulate a pro-inflammatory response, as evidenced by the upregulation of numerous pro-inflammatory genes. Upon exposure to hHL or ShHL, macrophages exhibited a difference and substantial increase in the secretion of pro-inflammatory cytokines, thereby highlighting the varied impact of the two derivatives on THP-1-derived macrophages. Overall, our results provide compelling evidence of the capacity of *Halomonas* levans to modulate the phenotype of human macrophages in vitro and serve as potent pro-inflammatory agents. To the best of our knowledge, this study represents the first investigation into the interaction of *Halomonas* levan polysaccharides with macrophages, thereby expanding our understanding of the immunomodulatory potential of this intriguing polysaccharide.

CRediT authorship contribution statement

Ella Peled: Methodology, Investigation, Formal analysis, Writing – original and revised drafts.

Selay Tornaci: Methodology, Investigation, Formal analysis, Writing – original and revised drafts.

Ivan Zlotver: Methodology and Formal analysis.

Arita Dubnika: Conceptualization, Resources, Funding acquisition.

Ebru Toksoy Öner: Conceptualization, Methodology, Writing – original and revised drafts, Supervision, Resources, Funding acquisition.

Alejandro Sosnik: Conceptualization, Methodology, Writing – original and revised drafts, Supervision, Resources, Funding acquisition.

Notes

The authors declare no competing financial interests.

Declaration of competing interest

The authors declare that they have no known competing financial interests or personal relationships that could have appeared to influence the work reported in this paper.

Data availability

Data will be made available on request.

Acknowledgments

This work was funded by M-ERA.NET “Bioactive injectable hydrogels for soft tissue regeneration after reconstructive maxillofacial surgeries (INJECT-BIO)” of the Ministry of Science and Technology of Israel (grant #317330-3), the Latvian Council of Science (grant # ES RTD/2020/14) and the Scientific and Technological Research Council of Turkey (TUBITAK) (grant #119N756). A.S. thanks the support of the Tamara and Harry Handelsman Academic Chair and the partial financial support of Technion and the Russell Berrie Nanotechnology Institute (RBNI, Technion). We thank Prof. Ariel Kaplan from the biology faculty at the Technion, for his assistant with the RNA isolation. Library preparation, sequencing, quality control, and differential expression analyses were conducted by the “Technion Genome Center”.

Appendix A. Supplementary data

Supplementary data to this article can be found online at https://doi.org/10.1016/j.carbpol.2023.121203.

References

Andrade, R. G. D., Reis, B., Costas, B., Lima, S. A. C., & Reis, S. (2021). Modulation of macrophages m1/m2 polarization using carbohydrate-functionalized polymeric nanoparticles. *Polymers, 13*(1), 1–18.

Arabpour, M., Saghazadeh, A., & Rezaei, N. (2021). Anti-inflammatory and M2 macrophage polarization-promoting effect of mesenchymal stem cell-derived exosomes. *International Immunopharmacology, 97*, Article 107823.

Aramsangtienchai, P., Kongmon, T., Pechroj, S., & Srisook, K. (2020). Enhanced production and immunomodulatory activity of levan from the acetic acid bacterium, Tanticharoenia sakaeratensis. *International Journal of Biological Macromolecules, 163*, 574–581.

Aramsangtienchai, P., Raksachue, W., Pechroj, S., & Srisook, K. (2023). The immunomodulatory activity of levan in RAW264.7 macrophage varies with its molecular weights. *Food Bioscience, 53*, Article 102721.

Avsar, G., Agirbasli, D., Agirbasli, M. A., Gunduz, O., & Oner, E. T. (2018). Levan based fibrous scaffolds electrospun via co-axial and single-needle techniques for tissue engineering applications. *Carbohydrate Polymers, 193*, 316–325.

Barron, L., & Wynn, T. A. (2011). Macrophage activation governs schistosomiasis-induced in- flammation and fibrosis. *Eur. J. Immunol., 41*, 2509–2514.

Baseler, W. A., Davies, L. C., Quigley, L., Ridnour, L. A., Weiss, J. M., Perwez Hussain, S., … McVicar, D. W. (2016). Autocrine IL-10 functions as a rheostat for M1 macrophage glycolytic commitment by tuning nitric oxide production. *Redox Biology, 10*, 12–23.

Campbell, L. M., Maxwell, P. J., & Waugh, D. J. J. (2013). Rationale and means to target pro-inflammatory interleukin-8 (CXCL8) signaling in cancer. *Pharmaceuticals, 6*(8), 929.

Cinan, E., Cesur, S., Haskoylu, M. E., Gunduz, O., & Oner, E. T. (2021). Resveratrol-loaded levan nanoparticles produced by electrohydrodynamic atomization technique. *Nanomaterials, 11*(10), 2582.

Combie, J., & Toksoy Öner, E. (2018). From healing wounds to resorbable electronics, levan can fill bioadhesive roles in scores of markets. *Bioinspiration & Biomimetics, 14*(1), Article 011001.

Correa-Gallegos, D., Jiang, D., & Rinkevich, Y. (2021). Fibroblasts as confederates of the immune system. *Immunological Reviews, 302*(1), 147–162.

de Siqueira, E. C., & Toksoy Öner, E. (2023). Co-production of levan with other high-value bioproducts: A review. *International Journal of Biological Macromolecules, 235*, Article 123800.

Dong, C. X., Zhang, L. J., Xu, R., Zhang, G., Zhou, Y. B., Han, X. Q., … Sun, Y. X. (2015). Structural characterization and immunostimulating activity of a levan-type fructan from Curcuma kwangsiensis. *International Journal of Biological Macromolecules, 77*, 99–104.

Erginer, M., Akcay, A., Coskunkan, B., Morova, T., Rende, D., Bucak, S., … Toksoy Oner, E. (2016). Sulfated levan from Halomonas smyrnensis as a bioactive, heparin-mimetic glycan for cardiac tissue engineering applications. *Carbohydrate Polymers, 149*, 289–296.

Erkorkmaz, B. A., Kırtel, O., Abaramak, G., Nikerel, E., & Toksoy Öner, E. (2022). UV and chemically induced Halomonas smyrnensis mutants for enhanced levan productivity. *Journal of Biotechnology, 356*, 19–29.
Feng, D., Huang, W. Y., Niu, X. L., Hao, S., Zhang, L. N., & Hu, Y. J. (2021). Significance of macrophage subtypes in the peripheral blood of children with systemic juvenile idiopathic arthritis. *Rheumatology and Therapy, 8*(4), 1859–1870.
Gakharia, T., Bakhtadze, S., Lim, M., Khachapuridze, N., & Kapanadze, N. (2022). Alterations of plasma pro-inflammatory cytokine levels in children with refractory epilepsies. *Children, 9*(10), 1506.
Genin, M., Clement, F., Fattaccioli, A., Raes, M., & Michiels, C. (2015). M1 and M2 macrophages derived from THP-1 cells differentially modulate the response of cancer cells to etoposide. *BMC Cancer, 15*(1), 1–14.
Gomes, T. D., Caridade, S. G., Sousa, M. P., Azevedo, S., Kandur, M. Y., Öner, E. T., … Mano, J. F. (2018). Adhesive free-standing multilayer films containing sulfated levan for biomedical applications. *Acta Biomaterialia, 69*, 183–195.
He, L., Jhong, J. H., Chen, Q., Huang, K. Y., Strittmatter, K., Kreuzer, J., … Marneros, A. G. (2021). Global characterization of macrophage polarization mechanisms and identification of M2-type polarization inhibitors. *Cell Reports, 37*(5), Article 109955.
Herb, M., Gluschko, A., Wiegmann, K., Farid, A., Wolf, A., Utermöhlen, O., Krut, O., Krönke, M., & Schramm, M. (2019). Mitochondrial reactive oxygen species enable proinflammatory signaling through disulfide linkage of NEMO. *Science Signaling, 12*(568), Article eaar5926.
Huang, L., Shen, M., Morris, G. A., & Xie, J. (2019). Sulfated polysaccharides: Immunomodulation and signaling mechanisms. *Trends in Food Science & Technology, 92*, 1–11.
Janse van Rensburg, H. C., Takács, Z., Freynschlag, F., Öner, E. T., Jonak, C., & Van den Ende, W. (2020). Fructans prime ROS dynamics and botrytis cinerea resistance in arabidopsis. *Antioxidants, 9*(9), 805.
Jung, S., Park, J., & Ko, K. S. (2020). Lipopolysaccharide-induced innate immune responses are exacerbated by Prohibitin 1 deficiency and mitigated by S-adenosylmethionine in murine macrophages. *PLoS One, 15*(11), Article e0241224.
Kirtel, O., Menéndez, C., Versluys, M., Van den Ende, W., Hernández, L., & Toksoy Öner, E. (2018). Levansucrase from Halomonas smyrnensis AAD6T: First halophilic GH-J clan enzyme recombinantly expressed, purified, and characterized. *Applied Microbiology and Biotechnology, 102*(21), 9207–9220.
Kirtel, O., & Öner, E. T. (2021). Levan polysaccharide for biomedical applications. *Soft Matter for Biomedical Application, 13*, 134.
Kırtel, O., Versluys, M., Van den Ende, W., & Toksoy Öner, E. (2018). Fructans of the saline world. *Biotechnology Advances, 36*(5), 1524–1539.
Koper-Lenkiewicz, O. M., Sutkowska, K., Wawrusiewicz-Kurylonek, N., Kowalewska, E., & Matowicka-Karna, J. (2022). Proinflammatory cytokines (IL-1, -6, -8, -15, -17, -18, -23, TNF-α) single nucleotide polymorphisms in rheumatoid arthritis—A literature review. *International Journal of Molecular Sciences, 23*(4), 2106.
Kumar, V. (2019). Macrophages: The potent immunoregulatory innate immune cells. In K. H. Bhat (Ed.), *Macrophage activation - Biology and disease*. IntechOpen.
Li, P., Hao, Z., Wu, J., Ma, C., Xu, Y., Li, J., Lan, R., Zhu, B., Ren, P., Fan, D., & Sun, S. (2021). Comparative proteomic analysis of polarized human THP-1 and mouse RAW264.7 macrophages. *Frontiers in Immunology, 12*, Article 700009.
Li, X. Y., Wang, Y. J., Chen, S., Pan, L. H., Li, Q. M., Luo, J. P., & Zha, X. Q. (2022). Laminaria japonica polysaccharide suppresses atherosclerosis via regulating autophagy-mediated macrophage polarization. *Journal of Agricultural and Food Chemistry, 70*(12), 3633–3643.
Li, Z., & Bratlie, K. M. (2021). The influence of polysaccharides-based material on macrophage phenotypes. *Macromolecular Bioscience, 21*(8), Article 2100031.
Liberzon, A., Birger, C., Thorvaldsdóttir, H., Ghandi, M., Mesirov, J. P., & Tamayo, P. (2015). The molecular signatures database hallmark gene set collection. *Cell Systems, 1*(6), 417–425.
Liberzon, A., Subramanian, A., Pinchback, R., Thorvaldsdóttir, H., Tamayo, P., & Mesirov, J. P. (2011). Molecular signatures database (MSigDB) 3.0. *Bioinformatics, 27*(12), 1739–1740.
Liu, J., Geng, X., Hou, J., & Wu, G. (2021). New insights into M1/M2 macrophages: Key modulators in cancer progression. *Cancer Cell International, 21*(1), 389.
Locati, M., Curtale, G., & Mantovani, A. (2020). Diversity, mechanisms, and significance of macrophage plasticity. *Annual Review of Pathology: Mechanisms of Disease, 15*, 123–147.
Love, M. I., Huber, W., & Anders, S. (2014). Moderated estimation of fold change and dispersion for RNA-seq data with DESeq2. *Genome Biology, 15*(12), 550.
Magri, A., Oliveira, M. R., Baldo, C., Tischer, C. A., Sartori, D., Mantovani, M. S., & Celligoi, M. A. P. C. (2020). Production of fructooligosaccharides by Bacillus subtilis natto CCT7712 and their antiproliferative potential. *Journal of Applied Microbiology, 128*(5), 1414–1426.
Miao, X., Leng, X., & Zhang, Q. (2017). The current state of nanoparticle-induced macrophage polarization and reprogramming research. *International Journal of Molecular Sciences, 18*(2), 336.
Mihailescu, N., Haskoylu, M. E., Ristoscu, C., Bostan, M. S., Sopronyi, M., Eroğlu, M. S., … Mihailescu, I. N. (2019). Gradient multifunctional biopolymer thin film assemblies synthesized by combinatorial MAPLE. *Applied Surface Science, 466*, 628–636.
Murray, P. J. (2017). Macrophage polarization. *Annual Review of Physiology, 79*(1), 541–566.
Murray, P. J., Allen, J. E., Biswas, S. K., Fisher, E. A., Gilroy, D. W., Goerdt, S., … Wynn, T. A. (2014). Macrophage activation and polarization: Nomenclature and experimental guidelines. *Immunity, 14*(1), 14–20.
Mutlu, E. C., Bahadori, F., Bostan, M. S., Sarilmiser, H. K., ToksoyOner, E., & Eroğlu, M. S. (2021). Halomonas levan-coated phospholipid-based nano-carrier for active targeting of A549 lung cancer cells. *European Polymer Journal, 144*, Article 110239.
Naik, E., & Dixit, V. M. (2011). Mitochondrial reactive oxygen species drive proinflammatory cytokine production. *The Journal of Experimental Medicine, 208*(3), 417.
Nakai, K. (2021). Multiple roles of macrophage in skin. *Journal of Dermatological Science, 104*(1), 2–10.
Osman, A., Lin, E., & Hwang, D. S. (2023). A sticky carbohydrate meets a mussel adhesive: Catechol-conjugated levan for hemostatic and wound healing applications. *Carbohydrate Polymers, 299*, Article 120172.
Peled, E., & Sosnik, A. (2021). Amphiphilic galactomannan nanoparticles trigger the alternative activation of murine macrophages. *Journal of Controlled Release, 339*, 473–483.
Pu, Y., Liu, Z., Tian, H., & Bao, Y. (2019). The immunomodulatory effect of Poria cocos polysaccharides is mediated by the Ca2+/PKC/p38/NF-κB signaling pathway in macrophages. *International Immunopharmacology, 72*, 252–257.
Rendra, E., Riabov, V., Mossel, D. M., Sevastyanova, T., Harmsen, M. C., & Kzhyshkowska, J. (2019). Reactive oxygen species (ROS) in macrophage activation and function in diabetes. *Immunobiology, 224*(2), 242–253.
Sica, A., & Mantovani, A. (2012). Macrophage plasticity and polarization: In vivo veritas. *Journal of Clinical Investigation, 122*(3), 787–795.
Song, Y., Zhang, H., Song, Z., Yang, Y., Zhang, S., & Wang, W. (2022). Levan polysaccharide from Erwinia herbicola protects osteoblast cells against lipopolysaccharide-triggered inflammation and oxidative stress through regulation of ChemR23 for prevention of osteoporosis. *Arabian Journal of Chemistry, 15*(4), Article 103694.
Sridharan, R., Cameron, A. R., Kelly, D. J., Kearney, C. J., & O'Brien, F. J. (2015). Biomaterial based modulation of macrophage polarization: A review and suggested design principles. *Materials Today, 18*(6), 313–325.
Subramanian, A., Tamayo, P., Mootha, V. K., Mukherjee, S., Ebert, B. L., Gillette, M. A., … Mesirov, J. P. (2005). Gene set enrichment analysis: A knowledge-based approach for interpreting genome-wide expression profiles. *Proceedings of the National Academy of Sciences U.S.A., 102*(43), 15545–15550.
Susan Van Dyk, J., Low, N., Kee, A., Frost, C. L., & Pletschke, B. I. (2012). Extracellular polysaccharides. *BioResources, 7*(4), 4976–4993.
Tamburrini, A., Colombo, C., & Bernardi, A. (2020). Design and synthesis of glycomimetics: Recent advances. *Medicinal Research Reviews, 40*(2), 495–531.
Tardito, S., Martinelli, G., Soldano, S., Paolino, S., Pacini, G., Patane, M., Alessandri, E., Smith, V., & Cutolo, M. (2019). Macrophage M1/M2 polarization and rheumatoid arthritis: A systematic review. *Autoimmunity Reviews, 18*(11), Article 102397.
Toksoy Öner, E., Hernández, L., & Combie, J. (2016). Review of Levan polysaccharide: From a century of past experiences to future prospects. *Biotechnology Advances, 34*(5), 827–844.
Trapnell, C., Roberts, A., Goff, L., Pertea, G., Kim, D., Kelley, D. R., … Pachter, L. (2012). Differential gene and transcript expression analysis of RNA-seq experiments with TopHat and Cufflinks. *Nat. Protoc., 7*, 562–578.
Versluys, M., Toksoy Öner, E., & Van Den Ende, W. (2022). Fructan oligosaccharide priming alters apoplastic sugar dynamics and improves resistance against Botrytis cinerea in chicory. *Journal of Experimental Botany, 73*(12), 4214–4235.
Vyshkina, T., Sylvester, A., Sadiq, S., Bonilla, E., Perl, A., & Kalman, B. (2008). CCL genes in multiple sclerosis and systemic lupus erythematosus. *Journal of Neuroimmunology, 200*(1–2), 145.
Wang, Y., Feng, Z., Liu, X., Yang, C., Gao, R., Liu, W., Ou-Yang, W., Dong, A., Zhang, C., Huang, P., & Wang, W. (2022). Titanium alloy composited with dual-cytokine releasing polysaccharide hydrogel to enhance osseointegration via osteogenic and macrophage polarization signaling pathways. *Regenerative Biomaterials, 9*, rbac003.
Wang, Y., Smith, W., Hao, D., He, B., & Kong, L. (2019). M1 and M2 macrophage polarization and potentially therapeutic naturally occurring compounds. *International Immunopharmacology, 70*, 459–466.
Wei, W., Li, Z. P., Bian, Z. X., Han, Q., & bin.. (2019). Astragalus polysaccharide RAP induces macrophage phenotype polarization to M1 via the notch signaling pathway. *Molecules, 24*(10), 2016.
Wu, C., Ge, J., Yang, M., Yan, Q., Wang, Y., Yu, H., Yang, H., & Zou, J. (2021). Resveratrol protects human nucleus pulposus cells from degeneration by blocking IL-6/JAK/STAT3 pathway. *European Journal of Medical Research, 26*(1), 2016.
Xijin Ge, S., Jung, D., & Yao, R. (2020). ShinyGO: A graphical gene-set enrichment tool for animals and plants. *Bioinformatics, 36*(8), 2628–2629.
Xu, Q., Yajima, T., Li, W., Saito, K., Ohshima, Y., & Yoshikai, Y. (2006). Levan (β-2, 6-fructan), a major fraction of fermented soybean mucilage, displays immunostimulating properties via Toll-like receptor 4 signalling: Induction of interleukin-12 production and suppression of T-helper type 2 response and immunoglobulin E production. *Clinical & Experimental Allergy, 36*(1), 94–101.
Xu, X., Gao, C., Liu, Z., Wu, J., Han, J., Yan, M., & Wu, Z. (2016). Characterization of the levan produced by Paenibacillus bovis sp. nov BD3526 and its immunological activity. *Carbohydrate Polymers, 144*, 178–186.
Young, I. D., Latousakis, D., & Juge, N. (2021). The immunomodulatory properties of β-2,6 fructans: A comprehensive review. *Nutrients, 13*(4), 1309.
Young, I. D., Nepogodiev, S. A., Black, I. M., Le Gall, G., Wittmann, A., Latousakis, D., … Kawasaki, N. (2022). Lipopolysaccharide associated with β-2,6 fructan mediates TLR4-dependent immunomodulatory activity in vitro. *Carbohydrate Polymers, 277*, Article 118606.
Yunna, C., Mengru, H., Lei, W., & Weidong, C. (2020). Macrophage M1/M2 polarization. *European Journal of Pharmacology, 877*, Article 173090.